scientific reports

OPEN

Glycolysis-related lncRNA FTX upregulates YAP1 to facilitate colorectal cancer progression via sponging miR-215-3p

Jin-Lan Yang[1,4,5], Jing-Jing Ma[2,5], Tian-Yin Qu[1,4], Qing Dai[1,4], Jing Leng[1,4], Lin Fang[1,4], Jie Wu[3], Ya-Jun Li[1] & Huang-Fei Yu[1,4]✉

Increased evidence reveals that glycolysis is one of the key metabolic hallmarks of cancer cells. However, the roles of lncRNA FTX in energy metabolism and cancer progression remain unclear. In this study we aim to show that lncRNA FTX was significantly upregulated in cancer tissues and serum of CRC patients and CRC cell lines. Function study indicated that it could promote aerobic glycolysis, cell proliferation, migration and invasion in colorectal cancer cells. Further mechanistic studies showed, lncRNA FTX was found to function as a sponge for miR-215-3p, which reduced the ability of miR-215-3p to repress the YAP1 oncoprotein. Additionally, a negative correlation was observed between lncRNA FTX and miR-215-3p expression, and the knockdown of lncRNA FTX or miR-215-3p overexpression yielded opposite effects. In conclusion, this study demonstrates that FTX could directly combine with miR-215-3p as a competitive endogenous RNA, thus promoting the aerobic glycolysis and progression of CRC in vitro and in vivo.

Keywords Colorectal cancer, Glycolysis, LncRNA FTX, MiR-215-3p, YAP1

Colorectal cancer (CRC) is a prevalent cancer with a rising incidence rate in China[1,2]. Despite substantial research and clinical advancements, there is still a lack of comprehensive understanding regarding predictable biomarkers for CRC metastasis and effective therapeutics[3,4]. The development and progression of CRC are influenced by a combination of genetic and environmental factors. However, the underlying mechanisms responsible for CRC pathogenesis remain largely unknown. Thus, further studies are necessary to identify crucial molecules involved in the growth and metastasis of CRC.

Alterations in cellular metabolism have been recognized as emerging hallmarks of cancer[5], with one of the well-recognized hallmarks being aerobic glycolysis, commonly known as the Warburg effect[6]. This phenomenon describes the preference of highly proliferative malignant cells to rely on glycolysis instead of oxidative phosphorylation, even in the presence of sufficient oxygen, to allow cancer cells to fulfill their high nutrient demands and sustain rapid proliferation[7,8]. Accumulating evidence suggests that the metabolic alterations associated with the Warburg effect play critical roles in tumor growth and progression[9,10]. Abnormal glycolysis, linked to the dysregulated expression of oncogenic molecules, contributes to the malignant progression of cancer[11,12]. Among these molecules, hypoxia-inducible factor 1 (HIF-1) is a key mediator of the Warburg effect. It can activate a cascade of genes involved in glucose metabolism, cell proliferation, migration and angiogenesis, such as Pyruvate Dehydrogenase Kinase (PDK), Lactate Dehydrogenase A (LDHA) and Vascular Endothelia Growth Factor (VEGF)[13]. Notably, the oncogene c-Myc transactivates several glycolytic genes, including Glucose Transporter 1 (GLUT1) and LDHA[14]. The tumor suppressor protein p53 could revert the Warburg effect, and to negatively influence the oncogenic metabolic adaption of cancer cells[15]. Those results reveal the important role of aberrant glucose metabolism in tumor progression due to oncogene expression.

[1]Department of Oncology, The First People's Hospital of Zunyi (The Third Affiliated Hospital of Zunyi Medical University), Zunyi 563000, Guizhou Province, China. [2]Department of Clinical Laboratory, The First People's Hospital of Zunyi (The Third Affiliated Hospital of Zunyi Medical University), Zunyi 563000, Guizhou Province, China. [3]Scientific Research Center, The First People's Hospital of Zunyi (The Third Affiliated Hospital of Zunyi Medical University, Zunyi 563000, Guizhou Province, China. [4]Cancer Disease Research Institute, The First People's Hospital of Zunyi (The Third Affiliated Hospital of Zunyi Medical University), 98# Fenghuang Road, Zunyi 563003, Guizhou Province, China. [5]Jing-Lan Yang and Jing-Jing Ma contributed equally to this work. ✉email: huangfeiyu@zmu.edu.cn

Yes-associated protein 1 (YAP1), a core component of the Hippo pathway, plays a crucial role as a transcriptional coactivator in regulating cellular processes such as proliferation, survival and self-renewal[16]. In numerous malignancies, including CRC, YAP1 is frequently overexpressed and considered an oncoprotein involved in tumor initiation and progression[17]. Previous studies have highlighted the close association between YAP1 and glucose homeostasis. For instance, in glucose-starved conditions, YAP1 has been reported to undergo phosphorylation and suppression by AMP-activated protein kinase (AMPK), while active YAP1 promoted glycolysis by enhancing glucose uptake and lactate production[18]. Moreover, YAP1 has been shown to suppress gluconeogenic gene expression through its interaction with PGC1a in hepatocellular carcinoma HepG2 cells. This newly discovered role of YAP1 in promoting the Warburg effect emphasizes the need for further investigation into its underlying mechanisms[19]. Thus, understanding these mechanisms is essential not only for gaining a better understanding of the role of YAP1 in regulating nutrient availability but also for assessing its translational potential as a target for YAP1-dependent glycolysis.

Long non-coding RNAs (lncRNAs) are a class of RNA molecules that are longer than 200 bases in length and cannot encode proteins. Recent evidence suggests that lncRNAs play a significant role in tumorigenesis and cancer progression[20,21]. One such lncRNA is five prime to Xist (FTX), which is a highly conserved transcript with 2300 nucleotides encoded by the *FTX* gene located on the human X chromosome inactivation region[22]. Several studies have demonstrated that FTX functions as an oncogene and is involved in the regulation of cancer progression in various types of cancers, including hepatocellular carcinoma[23,24], renal cell carcinoma[25], glioma[26], and CRC[27]. However, it remains unclear whether FTX can regulate glucose metabolism in cancer cells and act as an upstream regulator to stimulate YAP1 expression in CRC cells.

In this present study, we investigated the involvement of lncRNA FTX in CRC progression and its impact on glycometabolism. Our findings reveal that lncRNA FTX plays a significant role in promoting cell proliferation, invasion, migration, and facilitating glycolysis while inhibiting the tricarboxylic acid process in CRC by acting as an endogenous competing RNA of miR-215-3p to upregulate YAP1 expression. Overall, these findings highlight the functional importance of the lncRNA FTX-miR-215-3p-YAP1 axis in CRC and provide a novel mechanism to explain the progression of this disease.

Materials and methods

Blood samples and human CRC samples

The blood samples used in this study were collected from a total of 25 advanced CRC patients and 32 healthy individuals at The Third Affiliated Hospital of Zunyi Medical University (The First People's Hospital of Zunyi, Guizhou, China) between March 2021 and September 2021. The research protocol was approved by the Ethics Committee of The First People's Hospital of Zunyi (No. 2020-075), and written informed consent was obtained from all participants, all experiments were performed in accordance with relevant guidelines and regulations. Upon collection, all blood samples were immediately frozen and stored in liquid nitrogen until further use. The human CRC cDNA-HColA095Su02 chip (No: JSW-11-01) samples were obtained from Shanghai OUTDO Biotech Co., Ltd.

CRC cell line culture and culture conditions

Five human colonic adenocarcinoma cell lines, namely HT29, HCT116, SW480, SW620 and LOVO2, were acquired from the Cell Bank of the Chinese Academy of Sciences and cultured in RPMI-1640 medium (Gibco Cat#c11875500BT Carlsbad, CA, USA) supplemented with 10% fetal bovine serum (BI Cat#04-001-1ACS). Normal colon epithelial NCM-460 cell line was also obtained from BNCC (Cat# BNCC339288) and cultured in DMEM medium (Gibco Cat# C11995500BT) supplemented with 10% fetal bovine serum. All cell lines were maintained in a humidified cell incubator at 37 °C under an atmosphere of 5% CO_2.

Lentiviral transfections and construction of stable cell lines

The loss-of-function experiments were conducted by infecting HT29 cells with sh-FTX or sh-vector control lentivirus. The gain-of-function experiments were conducted by infecting HCT116 cells with Oe-FTX or Oe-vector control lentivirus obtained from JinHe Tech (Guizhou, China), at a multiplicity of infection of 10 μL with 10 mg/mL polybrene (JinHe Tech (Guizhou, China). Four days after the infection, puromycin-resistant cell lines were screened using a medium containing 2 μg/mL puromycin (Hanbio Tech Shanghai, China).

Plasmids, oligonucleotides, ShRNA, and transfection

MiR-215-3p mimic, negative control oligonucleotides (mimics NC), short hairpin RNA of YAP1 (sh-YAP1), and scramble shRNA (sh-NC) were synthesized by JinHe Tech (Guizhou, China). Briefly, the cells were seeded in six-well plates and allowed to culture overnight until reaching 60–70% confluence. The transfection was conducted using LipoFiter™ (Hanbio Tech Cat#HB-LF-1000, Shanghai, China) according to the manufacturer's instructions. All sequences of the shRNAs are listed in the Supplementary Table 1.

Real-time quantitative polymerase chain reaction (RT-qPCR)

The TRIzol reagent (Invitrogen; Thermo Fisher Scientific, Inc.) was used to isolate total RNA from cultured cells or serum samples. The isolated RNA (1 μg) was then reverse-transcribed into cDNA using an RT reagent kit (Takara Bio Cat#RR037A, Inc., Otsu, Japan) following the manufacturer's protocol based on the following conditions: 37 °C for 15 min, 85 °C for 5 s, and 4 °C for 10 min. Then, an SYBR Green PCR kit (Beijing Solarbio Science & Technology Co. Cat#SR1110, Ltd) and a LightCycler® 480 Real-Time PCR system was used for amplification. The instrument parameters were set as follows: pre-incubation at 95 °C for 10 min, followed by 39 cycles of denaturation at 95 °C for 20 s, annealing at 60 °C for 30 s, and extension at 72 °C for 30 s. The primer sequences used in this experiment are listed in Supplementary Table 1. The relative gene expression values were calculated using the $2^{-\Delta\Delta Cq}$ method, with GAPDH as the reference gene. To measure the level of miR-215-3p, a primer sequence designed and synthesized by RiboBio (Guangzhou, China) was used, with U6 snRNA serving as the endogenous control. All sequences of the primer pairs are listed in the Supplementary Table 2.

Cell proliferation assays

To perform the cell viability assay, CRC cells were seeded onto 96-well plates (1×10^4cells per well) after transfection. At 24,48, and 72 h post-transfection, 10 µL of Cell Counting Kit-8 (DOJINDO Cat#CK04, Japan) reagent was added to each well, followed by incubation for 2 h at 37 °C. The cell growth rate was determined by measuring the optical density (OD) at 450 nm using a plate reader (Bio-Rad, USA). For the colony formation assay, 1000 transfected cells were plated into each well of 6-well plates and cultured in a complete medium. After approximately 7–14 days, the cells were fixed with 4% paraformaldehyde and stained with 0.1% crystal violet for 30 min (Solarbio, Beijing, China). All experiments were repeated in triplicate, and the mean values were calculated.

Migration and invasion assays

For migration assay, 5×10^4 CRC cells were suspended in 100 µL of serum-free medium and seeded onto the membrane of the upper chamber of 24-well Transwell plates (Corning Cat#3422, NY, USA) at 48 h post-transfection. For the invasion assay, CRC cells (1×10^5) in serum-free media were placed into the upper chamber of Transwell plates pre-coated with Matrigel (Beijing Solarbio Science & Technology Co., Ltd). Following this, 500 µL of complete medium was added to the lower chamber. After 48 h, the cells on the upper membrane were gently removed by scraping with cotton wool. The cells on the lower membrane were fixed with 4% paraformaldehyde and stained with 0.1% crystal violet (Beijing Solarbio Science & Technology Co., Ltd). Microscopic observation and cell counting were performed to assess the extent of migration and invasion.

Measurement of lactate generation and detection of LDH

A total of 2×10^5 cells were seeded onto 6-well plates and cultured for 48 h, following which the culture medium was collected to measure lactate concentration using a lactate assay kit (Cat# KGT023; Nanjing KeyGen Biotech Co., Ltd., Nanjing, China). Then, the CRC cells were harvested to determine the protein concentration following the manufacturer's protocol. All lactate concentration values were normalized to their corresponding protein concentration values. Furthermore, the enzymatic activity levels of lactate dehydrogenase (LDH) were assessed using an LDH assay kit (Cat# A020-2) (all obtained from Nanjing Jiancheng Bioengineering Institute, Nanjing, China), according to the manufacturer's protocols.

Western blotting

The cells were lysed using radioimmunoprecipitation assay (RIPA) lysis solution containing 50 mM Tris-HCl (pH 7.4), 150 mM NaCl, 1% NP-40 and a complete protease inhibitor cocktail for 30 min on ice, followed by centrifugation at 12,000×g for 30 min at 4 °C. The protein concentration in the resulting lysates was determined using the BCA Protein Assay Kit (Cat# PC0020, Beijing Solarbio Science & Technology Co., Ltd). The cell extracts were then boiled for 10 min at 100 °C. Equal amounts of protein were separated by SDS-PAGE and transferred onto a polyvinylidene fluoride (PVDF) membrane (Millipore Cat#IPVH00010, Billerica, MA, USA), blocked in Western blocking buffer (Epizym, Shanghai, China) for 30 min at room temperature, followed by incubation with primary antibodies overnight at 4 °C. After three 5-minute washes with Tris-buffered saline solution containing Tween (TBST), the membranes were incubated with horseradish peroxidase (HRP)-conjugated secondary antibodies (Proteintech Cat#SA0001-1, WuHan, China) for 1 h at room temperature, and the protein bands were visualized using an enhanced chemiluminescence reagent (Epizym, Shanghai, China).

Luciferase reporter assay

To investigate the impact of miR-215-3p on LINC01123 or YAP1 3'-untranslated region (3'-UTR), HT29/HCT116 cells were transfected with individual wild-type (WT) and mutant-type (MUT) FTX and YAP1 3'-UTR reporter plasmids, along with 2 µg of mimics NC or miR-215-3p mimics. To confirm the competitive binding of miR-215-3p between lncRNA FTX and YAP1 3'-UTR, pcDNA-FTX or pcDNA-vector was co-transfected with miR-215-3p mimics and YAP1-3'-UTR-WT or YAP1-3'-UTR-MUT, respectively. After 24 h of transfection, firefly and Renilla luciferase activities were measured using the Dual-Luciferase Reporter Assay System (Promega Cat#E1910). The cell lysis fluid of the reporter gene served as a blank control. After determining firefly luciferase activity, 100 µL of the Renilla luciferase assay solution was added and homogenized. The relative light units (RLU) were measured using the GloMax 96 microplate luminometer, with Renilla luciferase as the internal reference. The RLU value obtained from the firefly luciferase measurement was divided by the RLU value obtained from the Renilla luciferase measurement. This ratio was used to assess the degree of gene activation and compare it between different samples.

Tumor xenografts

BALB/c nude mice were obtained from Beijing HFK Bio-Technology Co., Ltd. Stably transfected HT29 and HCT116 cells were used for in vivo experiments. Each mouse was injected subcutaneously with 1×10^7 cells into the left thigh ($n=6$ per group, randomized allocation). Tumor dimensions were measured every 2 days using digital calipers, and tumor volumes were calculated using the following formula: Volume (mm^3) = width^2(mm^2) × length (mm)/2, the tumor diameter is no more than 20 mm, and its volume is no more than 2000mm^3. After 4 weeks, the mice were euthanized (cervical dislocation) after being deeply anesthetized (pentobarbital sodium), dilute pentobarbital sodium with normal saline to a concentration of 1%, and administer 0.1–0.2 ml/10 g of the solution intraperitoneally to mice, then the tumors were collected and snap-frozen for further experimentation.

Immunohistochemical staining (IHC) was performed to assess tumor nodules histologically. All animal experiments were conducted in accordance with the guidelines approved by the Laboratory Animal Ethics Committee of the First People's Hospital of Zunyi Medical University.

IHC staining
CRC tissue samples were fixed overnight in 4% paraformaldehyde at room temperature and subsequently embedded in paraffin. Serial sections with a thickness of 5 μm were prepared. The sections were treated with hydrogen peroxide (3%) for 10 min to facilitate antigen retrieval and heated to 100 °C in citrate buffer for 8 min, then cooled to 25 °C. To block nonspecific binding, the sections were incubated in a humidified environment with 10% goat serum for 30 min. Subsequently, the sections were incubated overnight at 4 °C with primary antibodies, including YAP1 (1:100, Cat#13584-1-AP, Proteintech, Wuhan, China) and Ki-67 (1:200, Cat#AF0198, Affinity, China). The following day, the sections were incubated with anti-mouse HRP-conjugated secondary antibodies for 30 min at room temperature in a humid chamber, developed with diaminobenzidine tetrahydrochloride (DAB), stained with hematoxylin, and images were captured for further analysis.

Statistical analysis
Statistical analyses were performed using Graph Prism version 8.0 and SPSS 18.0. The data are presented as mean ± standard deviation (SD) from at least three independent replicates. Differences between experimental groups were assessed using one-way analysis of variance (ANOVA), or Student's t-test, as appropriate. Kaplan–Meier analysis and log-rank test were employed to analyze the relationship between lncRNA FTX expression and overall survival (OS) in the study population. Pearson correlation analysis was conducted to investigate the correlations between lncRNA FTX and miR-215-3p expressions and between miR-215-3p and YAP1 expressions. A significance level of $p < 0.05$ was considered statistically significant.

Results
Expression of LncRNA FTX in CRC patient's tissues, serum and cell lines
To investigate the role of lncRNA FTX in CRC, we analyzed the lncRNA expression profiles of CRC in the dataset GSE136735. A series of abnormally expressed lncRNAs in CRC were identified, and lncRNA FTX was upregulated lncRNAs (Fig. 1A). Meanwhile, we analyzed its expression in CRC tissues and adjacent normal colon tissues using bioinformatics based on data from The Cancer Genome Atlas (TCGA). Our analysis revealed that lncRNA FTX exhibited significantly higher expression levels in CRC tissues compared to normal colon tissues (Fig. 1B). Furthermore, Kaplan–Meier analysis indicated that high lncRNA FTX expression was associated with poor OS in 80 CRC patients ($P = 0.0026$) (Fig. 1C). Moreover, the area under the computed receiver operating characteristic (ROC) curve for lncRNA FTX was 0.718 (95% CI 0.658–0.778) (Fig. 1D), suggesting that upregulated lncRNA FTX could be a promising diagnostic marker for CRC patients. Subsequently, RT-qPCR was performed to assess lncRNA FTX expression in the serum of patients with advanced CRC, and the results demonstrated significantly higher lncRNA FTX expression in the patients' serum compared to normal healthy individuals (Fig. 1E). Additionally, lncRNA FTX exhibited higher expression in five CRC cell lines compared to the normal mucosal cells NCM-460 (Fig. 1F). Taken together, these findings suggest that lncRNA FTX acts as a cancer-promoting factor, as it is upregulated in CRC tissues and cell lines and could stimulate CRC growth and progression.

LncRNA FTX promotes cell proliferation, migration, invasion and aerobic glycolysis of CRC cells in vitro
To further investigate the role of lncRNA FTX in CRC cells, we constructed HT29 and HCT116 cell lines, which stably expressed low lncRNA FTX and high lncRNA FTX, respectively, through lentivirus infection. As shown in Fig. 2A, we observed that sh-FTX2 was more effective in downregulating lncRNA FTX expression in HT29 cells compared to sh-FTX1. Therefore, sh-FTX 2 was selected for subsequent experiments. CCK-8 assay demonstrated that the knockdown of lncRNA FTX significantly suppressed HT29 cell growth, whereas the overexpression of lncRNA FTX in HCT116 cells markedly stimulated cell proliferation compared to the control group (Fig. 2B). Similar trends were observed in the colony formation assay (Supplementary Fig. 1A). Furthermore, Transwell assay was performed to assess cell migration and invasion, and the results revealed that FTX downregulation weakened the migration and invasion abilities of HT29 cells, while in HCT116-oe-FTX cells significantly enhanced cell migration and invasion (Fig. 2C).

Aerobic glycolysis is a distinctive feature of malignant tumors. To evaluate the effect of lncRNA FTX on glycolysis, we detected LDH activity and lactic acid production and found that lncRNA FTX knockdown significantly reduced glycolysis capacity in HT29 cells, but the results were reversed following FTX overexpression (Fig. 2D). Moreover, the expression of Hexokinase 2 (HK2), Pyruvate kinase isozymetypeM2 (PKM2) and LDHA were significantly inhibited in HT29-sh-FTX cells, but could be remarkably increased in HCT116-oe-FTX cells (Fig. 2E). In HT29 cells with lncRNA FTX knockdown (HT29-shFTX cells), the expression of Citrate synthase (CS) and Isocitrate dehydrogenase 1 (IDH1), which are involved in the TCA cycle, was significantly enhanced. Conversely, in HCT116 cells with lncRNA FTX overexpression (HCT116-oeFTX cells), we observed a notable decrease in CS and IDH1 expression (Supplementary Fig. 1B). Taken together, these findings indicate that lncRNA FTX not only promotes malignant phenotypes such as proliferation, invasion and migration in CRC cells but also enhances glycolysis while inhibiting the metabolism of the tricarboxylic acid cycle.

LncRNA FTX regulates CRC growth in vivo
To further investigate the impact of lncRNA FTX on tumor growth, we conducted in vivo experiments using nude mice. As shown in Fig. 3A, the downregulation of FTX in HT29 cells significantly inhibited tumor formation

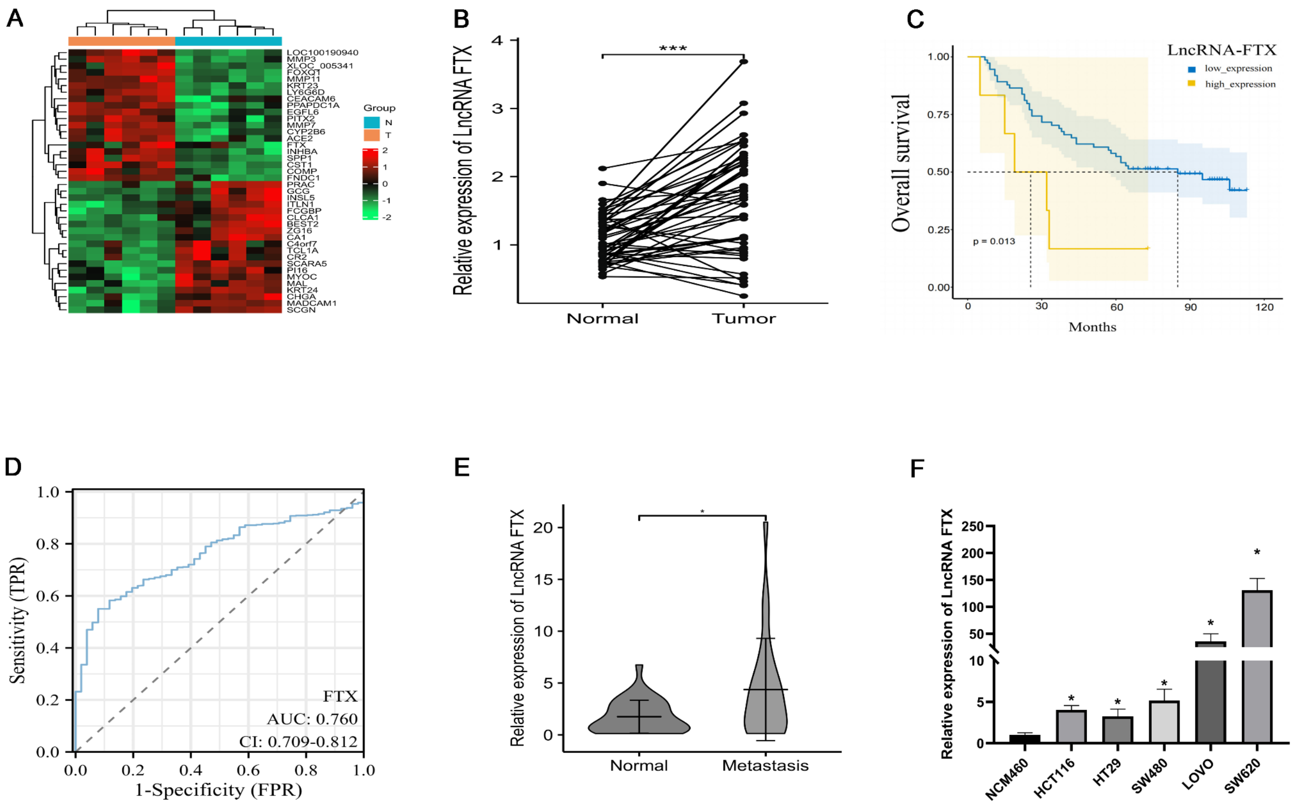

Fig. 1. LncRNA FTX is upregulated in colorectal cancer tissues and associated with poor prognosis in colorectal cancer patients. (**A**) Heatmap of most differentially expressed lncRNAs in GSE136735. (**B**) LncRNA FTX expression was validated by RT-qPCR in TCGA datasets (TCGA-COADREAD). (**C**) Kaplan–Meier survival analysis of overall survival in CRC patients according to lncRNA FTX expression. (**D**) Receiver operating characteristic curve (ROC) of the diagnostic validity of lncRNA FTX in TCGA datasets (TCGA-COADREAD). (**E**) RT-qPCR analysis of lncRNA FTX expression in serum samples of CRC patients ($n = 25$) and normal samples ($n = 32$). (**F**) Relative expression of lncRNA FTX in CRC cell lines and colon epithelial cell line. All representative data are from three independent experiments, and the results are presented as mean ± standard deviation. Statistical analysis was conducted using Student's t-test. *$p < 0.05$, **$p < 0.01$, ***$p < 0.001$.

and reduced tumor volume compared to the control group. Conversely, FTX overexpression in HCT116 cells significantly promoted tumor growth in nude mice (Fig. 3B). Immunohistochemical analysis of tumor tissues revealed that the number of Ki-67 positive cells, a marker of cancer cell proliferation, was lower in the HT29-sh-FTX group compared to the control group. In contrast, the HCT116-oe-FTX group exhibited a higher number of Ki-67 positive cells, indicating increased proliferation (Fig. 3C). Furthermore, we examined the expression of YAP1, a core molecule of the Hippo pathway known to promote tumor growth. In the HT29-sh-FTX group, YAP1 expression was inhibited in tumor tissues. Conversely, the HCT116-oe-FTX group exhibited higher expression levels of YAP1 (Fig. 3D). Collectively, these in vivo findings demonstrate that lncRNA FTX acts as an oncogenic factor that promotes CRC cell proliferation.

LncRNA FTX sequesters miR-215-3p to enhance CRC cell proliferation and aerobic glycolysis

To investigate the underlying molecular mechanism of lncRNA FTX in CRC, we used starbase2.0 to predict potential binding sites between lncRNA FTX and miR-215-3p (Fig. 4A). We found that miR-215-3p was downregulated in CRC patients, and its expression showed a negative correlation with lncRNA FTX ($r = -0.268$, $P < 0.001$) (Fig. 4B). In CRC cells, knockdown of lncRNA FTX in HT29 cells led to an increase in miR-215-3p expression, while overexpression of lncRNA FTX in HCT116 cells resulted in decreased miR-215-3p levels (Fig. 4C–D), indicating that miR-215-3p may function as a downstream target of lncRNA FTX and act as a tumor inhibitor in CRC. To further explore the role of miR-215-3p in CRC cells, we compared its expression in CRC cell lines to that in NCM460 cells using RT-qPCR, and observed lower expression of miR-215-3p in CRC cell lines (Supplementary Fig. 2A). To investigate the effects of miR-215-3p upregulation, we transfected miR-215-3p mimics into HT29 and HCT116 cells and observed a dramatic suppression of cell growth, migration and invasion (Supplementary Fig. 2B–E). Additionally, overexpression of miR-215-3p led to decreased LDH activity and lactate production in both HT29 and HCT116 cells (Supplementary Fig. 2F). Western blot analysis further revealed that the protein levels of HK2, LDH and PKM2 were significantly downregulated upon transfection of miR-215-3p mimics, while the expression of CS and IDH1, involved in the tricarboxylic acid cycle, was

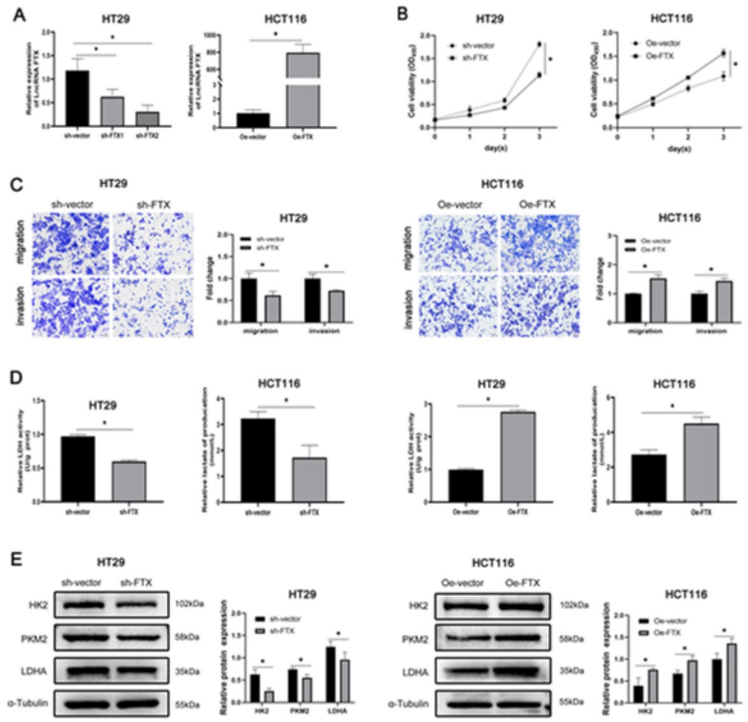

Fig. 2. LncRNA FTX promotes the proliferation and glycometabolism of CRC cells in vitro. (**A**) LncRNA FTX expression in HT29 cells transfected with shRNAs targeting lncRNA FTX and in HCT116 cells following lncRNA FTX overexpression via RT-qPCR. (**B**) Cell viability was determined using CCK-8 assay after transfection of sh-FTX and oe-FTX. (**C**) Cell migration and invasion was detected using Transwell assay after transfection of sh-FTX and oe-FTX. (**D**) Enzymatic activity levels of LDH and Lactate production were determined using corresponding assay kits when HT29 and HCT116 cells were transfected. (**E**) Protein expression levels of HK2, PKM2 and LDHA by western blot. The mean and standard error of the mean of three independent experiments performed in triplicate. *$p < 0.05$. Data are expressed as mean ± standard deviation; *t*-test was used to analyze data. HK2, Hexokinase 2; PKM2, Pyruvate kinase isozyme type M2; LDHA, Lactate dehydrogenase A. sh, short hairpin. CS, citrate synthase; IDH1, isocitrate dehydrogenase 1.

significantly upregulated (Supplementary Fig. 2G–H). These findings demonstrate that miR-215-3p functions as a tumor suppressor, inhibiting cancer progression and suppressing the Warburg effect in CRC cells.

To confirm the interaction between lncRNA FTX and miR-215-3p, a dual-luciferase reporter gene assay was performed. The results showed that co-transfection of the miR-215-3p mimic significantly attenuated the luciferase activity of the pGL3-lncRNA FTX-WT construct in both HT29 and HCT116 cells, while the miR-215-3p mimic did not affect the luciferase activity of the pGL3-lncRNA FTX-MUT construct (Fig. 4E). This indicates that lncRNA FTX acts as a direct sponge for miR-215-3p in CRC. Then, rescue experiments were conducted to further evaluate the impact of lncRNA FTX and miR-215-3p in CRC cells. In HCT116 cells, overexpression of miR-215-3p counteracted the effects of lncRNA FTX on cell proliferation, migration and invasion in CRC cells (Fig. 4F–H), the protein levels of YAP1 increased with lncRNA FTX overexpression, while the miR-215-3p partially attenuated the induction of YAP1 and c-Myc expression (Fig. 4I). Furthermore, the elevated lactate production and LDH enzyme activity induced by lncRNA FTX were reversed, along with the expression of proteins associated with aerobic glycolysis and the tricarboxylic acid cycle (Supplementary Fig. 3A–C).

YAP1 is a direct target of the LncRNA FTX/miR-215-3p signal axis

To investigate the downstream pathways of the lncRNA FTX/miR-215-3p axis, we used bioinformatics tools such as TargetScan Human (http://www.targetscan.org) and miRBase (https://www.mirbase.org) to determine whether YAP1 might be a potential target of miR-215-3p (Fig. 5A). YAP1, a transcriptional coactivator, plays significant roles in regulating tumor progression and energy metabolism in cancer cells. Consistent with numerous studies, including our previous research[28], YAP1 has been reported to be highly expressed in CRC tissue. Further analysis revealed a positive correlation between YAP1 and lncRNA FTX expression in CRC tissues ($r = 0.338$, $P < 0.001$) (Fig. 5B), as well as a negative correlation between YAP1 and miR-215-3p expression ($r = -0.306$ $P < 0.001$) (Fig. 5C). To explore the role of YAP1 on malignant proliferation and glucose metabolism of CRC cells, we transfected the cells with sh-YAP1 and sh-NC (Supplementary Fig. 4A). The results showed that the downregulation of YAP1 significantly inhibited cell proliferation, migration, and invasion in both HT29 and HCT116 cells (Supplementary Fig. 4B–D). Moreover, YAP1 knockdown suppressed lactate production and LDH

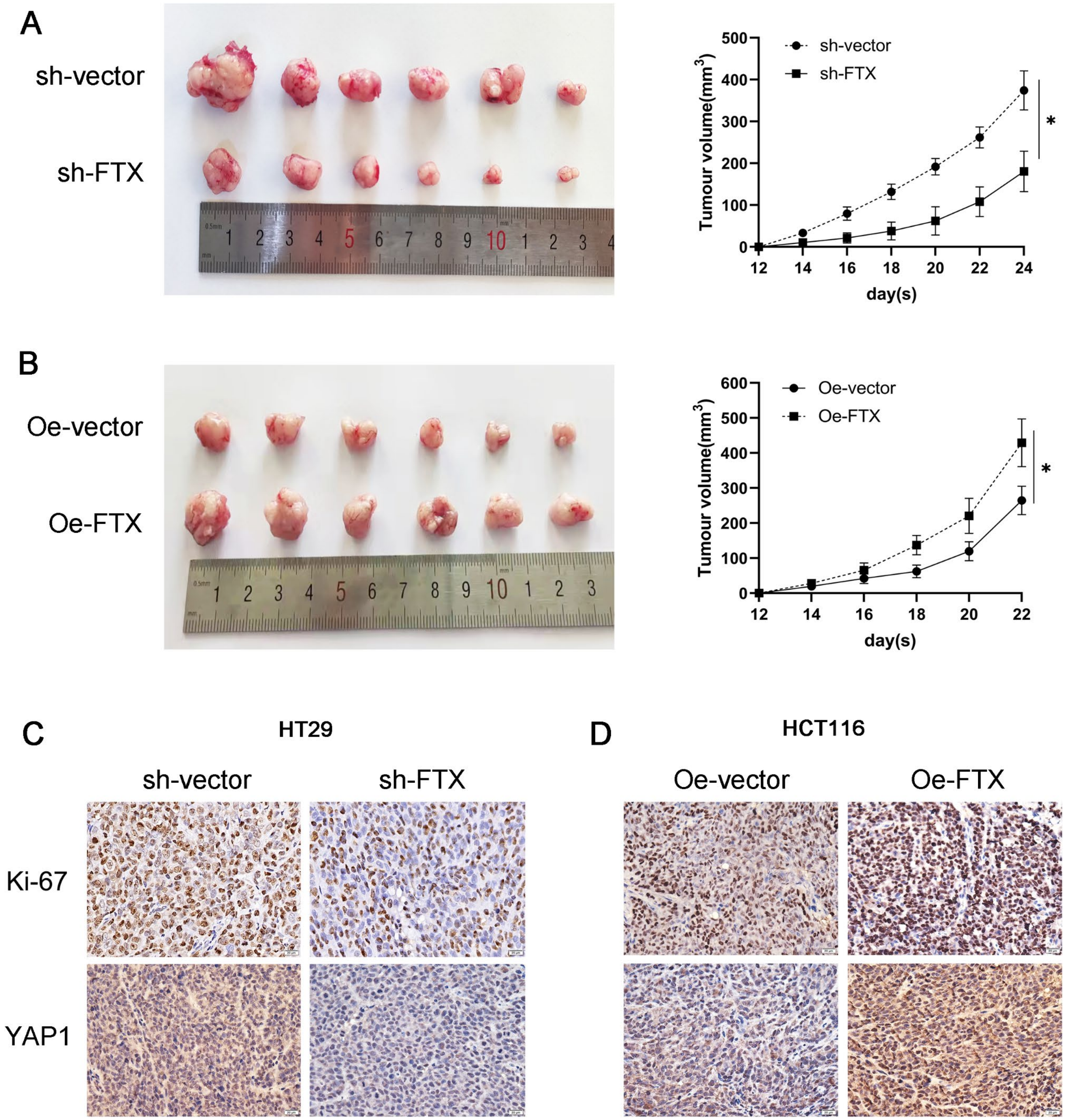

Fig. 3. LncRNA FTX regulates CRC growth in vivo. (**A**) Representative photographs of the tumors formed by HT29-sh-FTX or control cells subcutaneous vaccination (left). Tumor volume in xenograft mice injected with HT29-sh-FTX or control cells at the indicated times (right). (**B**) Representative photographs of the tumors formed by HCT116-FTX or control cells at harvest (left). Tumor volume in xenograft mice injected with HCT116-FTX or control cells at the indicated times (right). (**C**) Representative IHC staining images of YAP1 and Ki-67 in subcutaneous tumor xenograft tissues. Scale bar, 20 µm. (**D**) The expression of YAP1 and Ki-67 markers in HCT116-FTX and HCT116-vector xenograft tumors. Data are expressed as mean ± SD. $^{*}p < 0.05$.

activity in these cells (Supplementary Fig. 4E). Additionally, the expression levels of HK2, LDH, and PKM2, which are associated with glycolysis, were reduced upon YAP1 knockdown, while the expression levels of CS and IDH1, which are involved in the tricarboxylic acid cycle, were significantly enhanced (Supplementary Fig. 4F). Conversely, overexpression of YAP1 using the 5SA-YAP1 plasmid resulted in opposite effects in cancer cells (Supplementary Fig. 5A-F).

To further demonstrate that YAP1 is a downstream target of the lncRNA FTX/miR-215-3p signaling pathway, we examined the expression of YAP1 and its downstream target c-Myc in HT29-sh-FTX and HCT116-oe-FTX

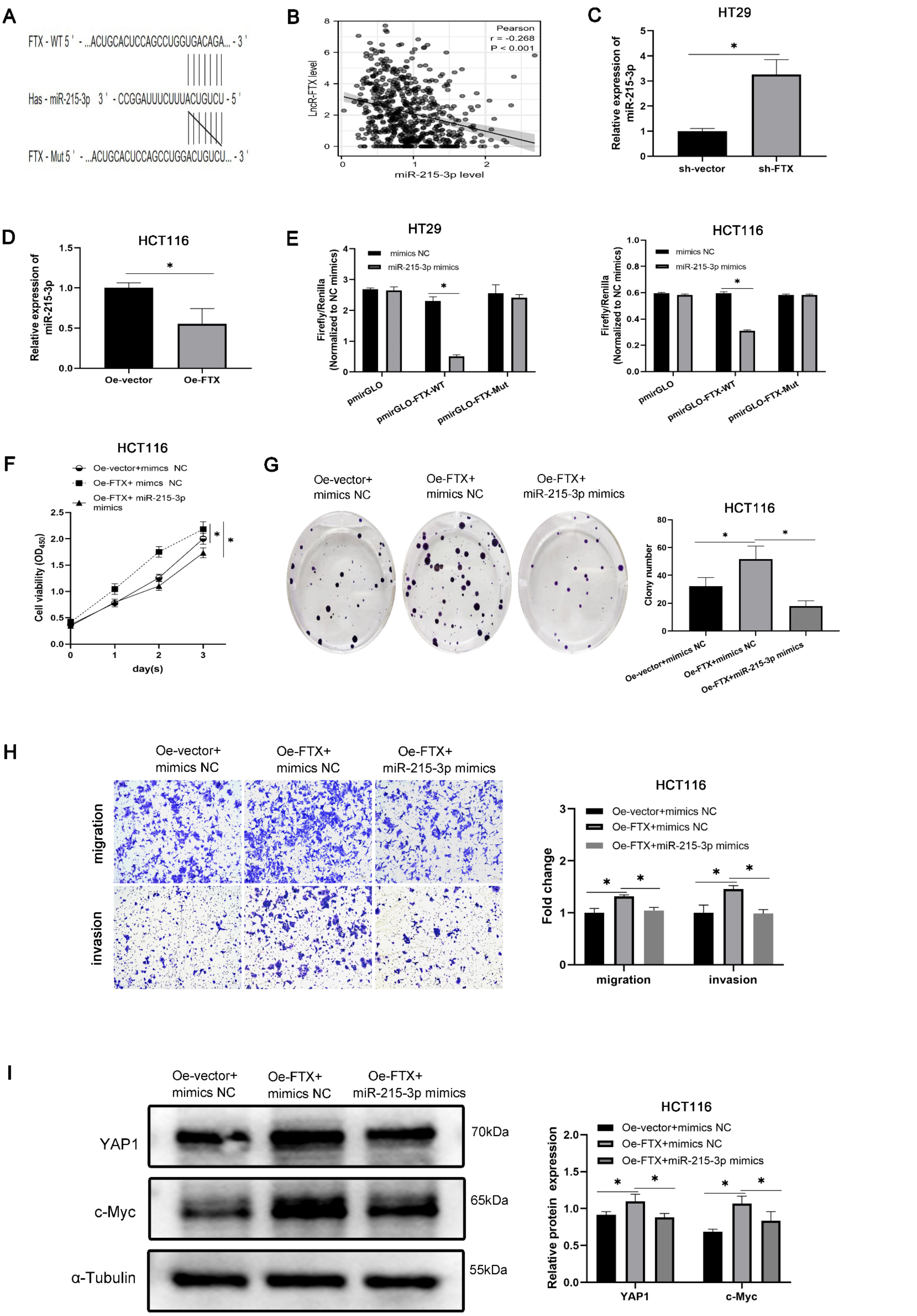

Fig. 4. LncRNA FTX sequester miR-215-3p to enhance colorectal cancer cell proliferation and aerobic glycolysis. (**A**) The potential binding site between lncRNA FTX and miR-215-3p predicted by Starbase. (**B**) Pearson's correlation analysis was performed to determine the correlation between lncRNA FTX and miR-215-3p expression. (**C**–**D**) miR-215-3p expression levels in FTX-depleted HT29 cells (**C**), and (**D**) FTX-overexpressing in HCT116 cells, in the corresponding control cells determined by RT-qPCR. (**E**) The targeting relationship between lncRNA FTX and miR-215-3p was confirmed by dual-luciferase reporter assay. (**F**–**G**) Growth inhibition evaluated by CCK-8 (**F**) and colony formation (**G**) assays in the indicated cells. (**H**) Transwell invasion assay of the cells described in. (**I**) Western blot analyses were performed to determine YAP1 and c-Myc expression after miR-215-3p upregulation in HCT116 cells overexpressing lncRNA FTX. *$p < 0.05$. Data are expressed as mean ± SD; *t*-test or ANOVA was used to analyze data.

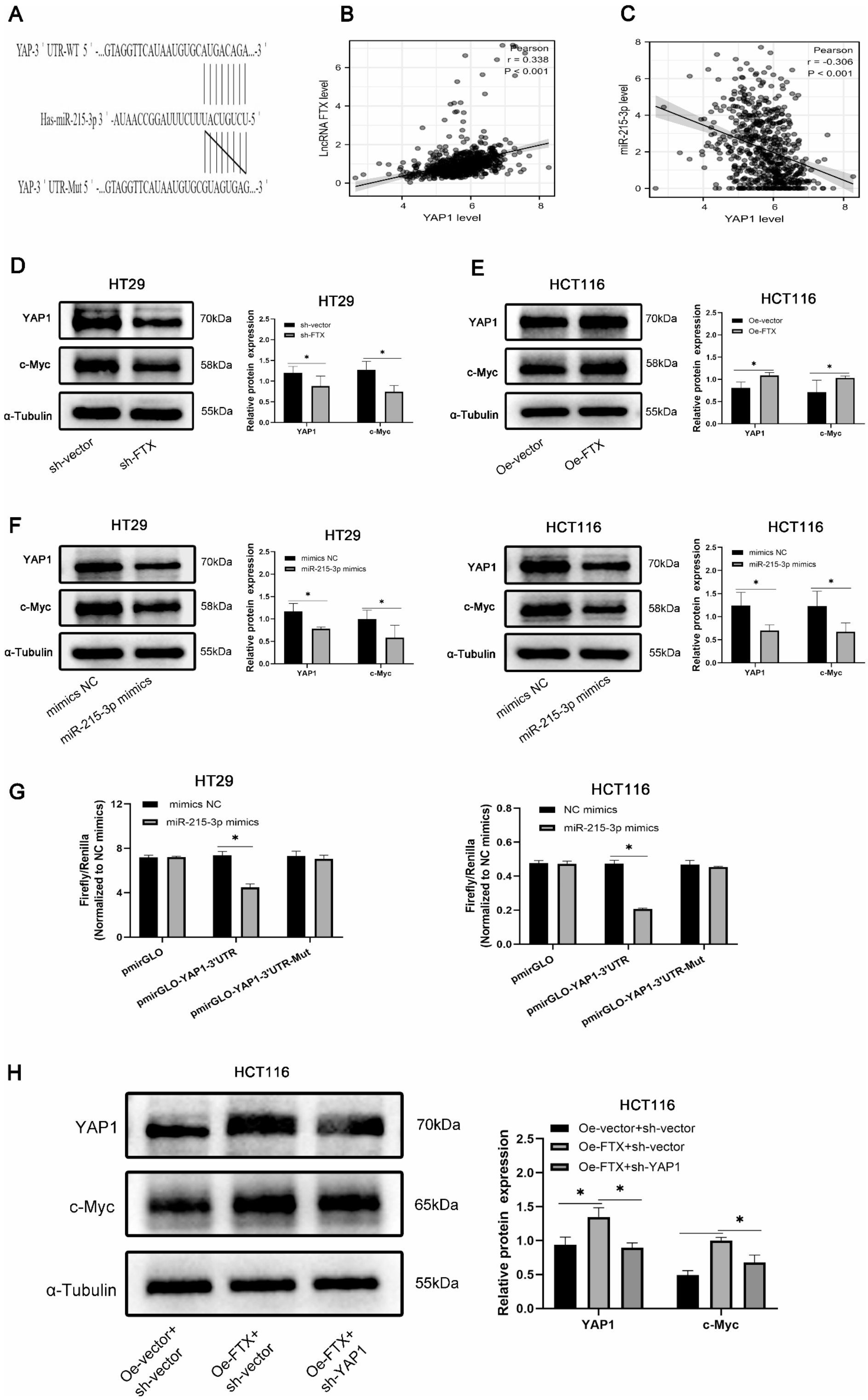

Fig. 5. YAP1 is a direct target of the lncRNA FTX/miR-215-3p signaling axis. (**A**) The potential binding site between miR-215-3p and YAP1 was predicted by the TargetScan database. (**B**) Pearson's correlation analysis was performed to determine the correlation between lncRNA FTX and YAP1 expression. (**C**) The correlation between miR-215-3p and YAP1 expression was analyzed by Pearson's correlation analysis. (**D**–**E**) The expression levels of YAP1 and c-Myc in HT29-sh-FTX (**D**) and HCT116-FTX cells (**E**) by western blotting. (**F**) Protein expression levels of YAP1 and c-Myc in miR-215-3p-overexpressing HT29 and HCT116 cells, respectively, and in the corresponding control cells, were determined by western blotting. (**G**) The targeting relationship between miR-215-3p and YAP1 was confirmed by dual-luciferase reporter assay in HT29 and HCT116 cells. (**H**) The expression levels of YAP1 and c-Myc markers in FTX-overexpressing HCT116 cells with or without transfection of shRNA targeting YAP1 and in the corresponding control cells were determined by western blotting. *$p < 0.05$. Data are expressed as mean ± SD; *t*-test or ANOVA was used to analyze data.

cells using RT-qPCR. The results showed that YAP1 and c-Myc expression significantly decreased in HT29 cells with FTX knockdown and increased in HCT116 cells with FTX overexpression (Fig. 5D–E). Additionally, when cells were transfected with the miR-215-3p mimic, YAP1 and c-Myc expression significantly decreased compared to cells transfected with the negative control mimic (Fig. 5F). We then constructed YAP1 full-length 3'-UTR reporters containing the predicted binding site of miR-215-3p and a mutant version of the site. Luciferase assays confirmed that the overexpression of the miR-215-3p mimic reduced the luciferase activity of the WT YAP1 reporter, but not the MUT reporter (Fig. 5G), indicating that YAP1 is a direct target of miR-215-3p. Furthermore, the protein levels of YAP1 increased with lncRNA FTX overexpression, but the shYAP1 partially attenuated the induction of YAP1 and c-Myc expression by lncRNA FTX in HCT116 cells during the rescue experiments (Fig. 5H). Downregulation of YAP1 in these cells rescued the promotive effects of lncRNA FTX on cell proliferation, migration, invasion, and aerobic glycolysis, while stimulating tricarboxylic acid metabolism (Supplementary Fig. 6A–E). These results suggest that YAP1 is a target of miR-215-3p in CRC and that lncRNA FTX regulates YAP1 expression by targeting miR-215-3p, thereby influencing the malignant properties and metabolic reprogramming of CRC cells.

Discussion

CRC is a devastating disease with complex yet unclear physiopathology. Previous studies have identified important genetic alterations in CRC, but targeting these genes for therapy has been challenging[29]. Recently, lncRNAs have emerged as valuable diagnostic and therapeutic targets in clinical oncology[30,31], some lncRNAs have shown promise as diagnostic or prognostic markers in various tumors[32,33]. For instance, LncRNA D16366 has been recognized as a prognostic marker for hepatocellular carcinoma[34]. While in breast cancer patients, lncRNA H19 has been identified as a potential diagnostic parameter and impaired the efficacy of chemo and radiotherapy in cancer cells[35,36]. Building on these findings, our research group verified the upregulation of lncRNA FTX expression in CRC and subsequently confirmed the suppression of CRC glycolysis and tumorigenesis by silencing lncRNA FTX. Mechanistically, lncRNA FTX sequesters miR-215-3p and releases its repression on YAP1, driving the Warburg effect and malignant progression of CRC. The results of our study provide novel evidence linking lncRNA FTX to CRC progression and support its potential as a prognostic biomarker in this disease.

There are two main approaches for the potential regulatory relationship between lncRNAs and their target proteins. The first is through complementary binding of the 3'-UTR region of microRNAs, which relieves the inhibition of target proteins by microRNAs. This mechanism is commonly referred to as competitive endogenous RNAs (ceRNAs)[37]. For example, in lung cancer, lncRNA JPX acts as an internal sponge to reduce the expression of miR-33a-5p[38]. Another example is lncRNA MALAT1, which acts as a ceRNA by directly binding to miR-200c and decreasing its expression in endometrioid endometrial carcinoma[39]. The second approach involves lncRNAs directly targeting the transcriptional sequence of downstream genes to regulate intracellular pathophysiological changes[40]. In hepatocellular carcinoma, lncRNA FTX promotes tumor progression and aerobic glycolysis by affecting PPAR. Studies have also found that lncRNA FTX can directly bind to MCM2 to prevent DNA replication and cancer cell proliferation[23]. Interestingly, FTX can be simultaneously involved in tumor progression through these two different mechanisms. In SW480 cells, Yang et al. reported that lncRNA FTX promotes the transcription of several downstream genes such as ZEB2, HOXB9 and NOB1 by sponging miR-215 and also directly binds to the mRNA of vimentin complementarily to influence its phosphorylation level at the Ser83 site[41]. These diverse findings suggest that FTX has a complex and significant function in tumors and may regulate the biological behavior of cancer cells through different molecular mechanisms, even within the same cell.

In the present study, we observed a negative correlation between lncRNA FTX and miR-215-3p in CRC cells. Depletion of lncRNA FTX suppressed the proliferation, migration, and glycolysis of CRC cells, and this promote effect was weakened upon the addition of the miR-215-3p. These findings suggest that lncRNA FTX exerts its function through miR-215-3p in CRC cells. MiR-215-3p has been recognized as an important suppressor in various cancers, including gastric cancer[42,43], lung adenocarcinoma[44] and cervical cancer[45], and overexpression of miR-215-3p has been shown to sensitize CRC cells to 5-Fu-induced apoptosis through the regulation of CXCR1[46]. Our results also revealed that miR-215-3p restricts YAP1 expression in CRC cells, while decreased miR-215-3p levels led to increased YAP1 expression. YAP1, as an oncogenic protein in the classical Hippo pathway, plays a crucial role in promoting aerobic glycolysis in hepatocellular carcinoma cells[47]. In hypoxic pancreatic ductal adenocarcinoma (PDAC), it has been reported that YAP1 recruits to the PKM2 gene promoter, resulting in the induction of glucose uptake, lactate production, and clonogenicity of cancer cells[48]. Indeed, the relationship between FTX and YAP1 was also confirmed in the DEPMAP database, both of which were highly expressed in colorectal cancer cells and cell survival was significantly suppressed after knocking down YAP1 using CRISPR or RNAi. In our experiment, we confirmed that the regulation of LncRNA/YAP1 could govern glycolysis and tricarboxylic acid metabolism in CRC cells.

Our study demonstrated that lncRNA FTX is highly expressed in CRC tissues and plays a crucial role in promoting CRC progression through the lncRNA FTX-miR-215-3p-YAP1 regulatory axis (Fig. 6). This research highlights the significant regulatory function of lncRNA FTX on the oncoprotein YAP1 in tumor cells and sheds light on the potential therapeutic targeting of lncRNA FTX in CRC treatment.

Conclusion

In conclusion, our study demonstrated that lncRNA FTX is highly expressed in CRC tissues and plays a crucial role in promoting CRC progression through the lncRNA FTX-miR-215-3p-YAP1 regulatory axis. This research highlights the significant regulatory function of lncRNA FTX on the oncoprotein YAP1 in tumor cells and sheds light on the potential therapeutic targeting of lncRNA FTX in CRC treatment.

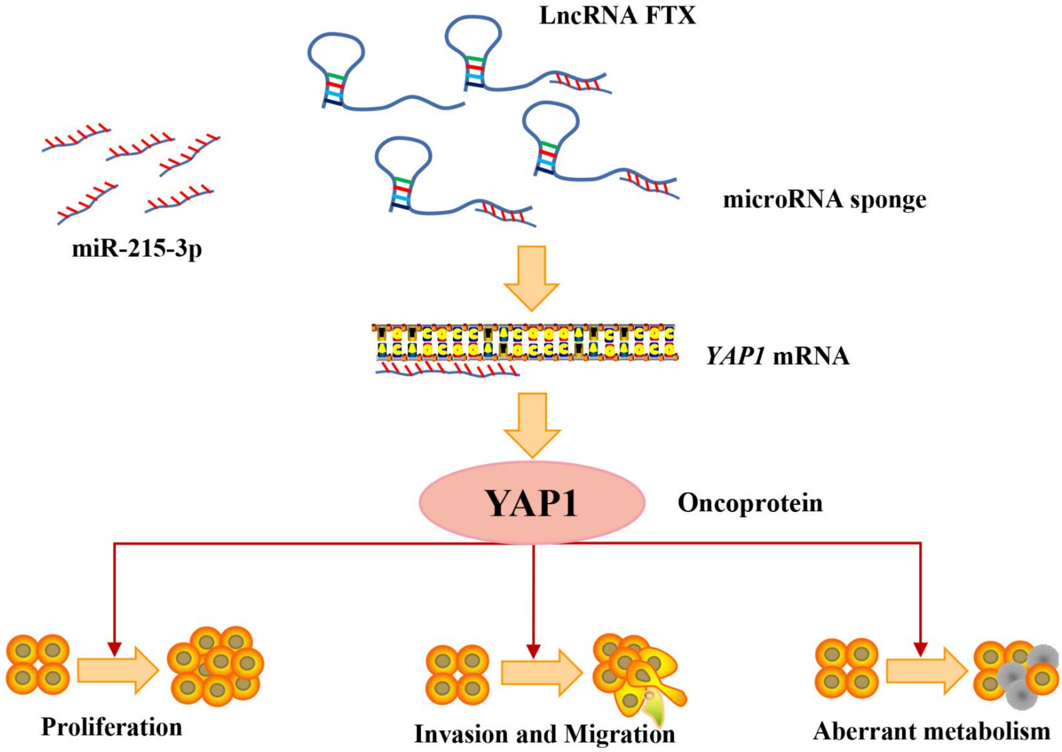

Fig. 6. A model of the role of LncRNA FTX in colorectal cancer progression and aerobic glycolysis.

Limitations of the study

We have shown that lncRNA FTX promotes CRC malignant biological behavior through lncRNA FTX-miR-215-3p-YAP1 regulatory axis. However, there are some shortcomings in this study, we lack animal validation and further evidence that YAP1 regulates key transcription factors in glycolysis.

Data availability

The data used for bioinformatic analyses were obtained from TCGA at TCGA-COADREAD and Gene Expression Omnibus (GEO) at GSE136735. The data are available from the corresponding author on reasonable request.

Received: 13 October 2024; Accepted: 17 March 2025
Published online: 22 March 2025

References

1. Qiu, H., Cao, S. & Xu, R. Cancer incidence, mortality, and burden in China: A time-trend analysis and comparison with the united States and united Kingdom based on the global epidemiological data released in 2020. *Cancer Commun. (Lond)*. **41** (10), 1037–1048 (2021).
2. Xia, C. et al. Cancer statistics in China and united States, 2022: Profiles, trends, and determinants. *Chin. Med. J. (Engl)*. **135** (5), 584–590 (2022).
3. Dienstmann, R. et al. Consensus molecular subtypes and the evolution of precision medicine in colorectal cancer. *Nat. Rev. Cancer* **17** (2), 79–92 (2017).
4. Kyrochristos, I. D. & Roukos, D. H. Comprehensive intra-individual genomic and transcriptional heterogeneity: Evidence-based colorectal cancer precision medicine. *Cancer Treat. Rev.* **80**, 101894 (2019).
5. Park, J. H., Pyun, W. Y. & Park, H. W. Cancer metabolism: phenotype, signaling and therapeutic targets. *Cells* **9** (10), 2308 (2020).
6. Fukushi, A., Kim, H. D., Chang, Y. C. & Kim, C. H. Revisited metabolic control and reprogramming cancers by means of the Warburg effect in tumor cells. *Int. J. Mol. Sci.* **23** (17), 10037 (2022).
7. Iacobini, C., Vitale, M., Pugliese, G. & Menini, S. The sweet path to cancer: Focus on cellular glucose metabolism. *Front. Oncol.* **13**, 1202093 (2023).
8. Comandatore, A. et al. Lactate dehydrogenase and its clinical significance in pancreatic and thoracic cancers. *Semin Cancer Biol.* **86** (Pt 2), 93–100 (2022).
9. Xu, J. Q. et al. Targeting Glycolysis in non-small cell lung cancer: Promises and challenges. *Front. Pharmacol.* **13**, 1037341 (2022).
10. Dyrstad, S. E. et al. Blocking aerobic glycolysis by targeting pyruvate dehydrogenase kinase in combination with EGFR TKI and ionizing radiation increases therapeutic effect in non-small cell lung cancer cells. *Cancers (Basel)* **13** (5), 941 (2021).
11. Feng, J. et al. Emerging roles and the regulation of aerobic glycolysis in hepatocellular carcinoma. *J. Exp. Clin. Cancer Res.* **39** (1), 126 (2020).
12. Abdel-Wahab, A. F., Mahmoud, W. & Al-Harizy, R. M. Targeting glucose metabolism to suppress cancer progression: Prospective of anti-glycolytic cancer therapy. *Pharmacol. Res.* **150**, 104511 (2019).

13. Sharma, A., Sinha, S. & Shrivastava, N. T. Targeting Hypoxia-Inducible factor (HIF-1) in cancer: Cutting gordian knot of cancer cell metabolism. *Front. Genet.* **13**, 849040 (2022).
14. Jing, Z. et al. NCAPD3 enhances Warburg effect through c-myc and E2F1 and promotes the occurrence and progression of colorectal cancer. *J. Exp. Clin. Cancer Res.* **41** (1), 198 (2022).
15. Gomes, A. S., Ramos, H., Soares, J. & Saraiva, L. p53 and glucose metabolism: An orchestra to be directed in cancer therapy. *Pharmacol. Res.* **131**, 75–86 (2018).
16. Zhao, B., Tumaneng, K. & Guan, K. L. The Hippo pathway in organ size control, tissue regeneration and stem cell self-renewal. *Nat. Cell. Biol.* **13** (8), 877–883 (2011).
17. Zanconato, F., Cordenonsi, M. & Piccolo, S. YAP/TAZ at the roots of cancer. *Cancer Cell.* **29** (6), 783–803 (2016).
18. DeRan, M. et al. Energy stress regulates hippo-YAP signaling involving AMPK-mediated regulation of angiomotin-like 1 protein. *Cell. Rep.* **9** (2), 495–503 (2014).
19. Hu, Y. et al. YAP suppresses gluconeogenic gene expression through PGC1α. *Hepatology* **66** (6), 2029–2041 (2017).
20. Singh, D. D., Lee, H. J. & Yadav, D. K. Recent clinical advances on long non-coding rNAs in triple-negative breast cancer. *Cells* **12** (4), 674 (2023).
21. Wu, Y. & Xu, X. Long non-coding RNA signature in colorectal cancer: Research progression and clinical application. *Cancer Cell. Int.* **23** (1), 28 (2023).
22. Chureau, C. et al. Ftx is a non-coding RNA which affects xist expression and chromatin structure within the X-inactivation center region. *Hum. Mol. Genet.* **20** (4), 705–718 (2011).
23. Liu, F. et al. Long noncoding RNA FTX inhibits hepatocellular carcinoma proliferation and metastasis by binding MCM2 and miR-374a. *Oncogene* **35** (41), 5422–5434 (2016).
24. Wu, H. et al. LncRNA FTX represses the progression of non-alcoholic fatty liver disease to hepatocellular carcinoma via regulating the M1/M2 polarization of Kupffer cells. *Cancer Cell. Int.* **20**, 266 (2020).
25. He, X. et al. Knockdown of long noncoding RNA FTX inhibits proliferation, migration, and invasion in renal cell carcinoma cells. *Oncol. Res.* **25** (2), 157–116 (2017).
26. Zhang, W. et al. Long noncoding RNA FTX is upregulated in gliomas and promotes proliferation and invasion of glioma cells by negatively regulating miR-342-3p. *Lab. Invest.* **97** (4), 447–457 (2017).
27. Yang, J., Qu, T., Li, Y., Ma, J. & Yu, H. Biological role of long non-coding RNA FTX in cancer progression. *Biomed. Pharmacother.* **153**, 113446 (2022).
28. Yu, H., Qu, T., Yang, J. & Dai, Q. Serotonin acts through YAP to promote cell proliferation: Mechanism and implication in colorectal cancer progression. *Cell. Commun. Signal.* **21** (1), 75 (2023).
29. Liu, Z. et al. Regulatory network and targeted interventions for CCDC family in tumor pathogenesis. *Cancer Lett.* **565**, 216225 (2023).
30. Liu, H., Luo, J., Luan, S., He, C. & Li, Z. Long non-coding RNAs involved in cancer metabolic reprogramming. *Cell. Mol. Life Sci.* **76** (3), 495–504 (2019).
31. Ahmad, M., Weiswald, L. B., Poulain, L., Denoyelle, C. & Meryet-Figuiere, M. Involvement of LncRNAs in cancer cells migration, invasion and metastasis: Cytoskeleton and ECM crosstalk. *J. Exp. Clin. Cancer Res.* **42** (1), 173 (2023).
32. Huang, Z., Zhang, M., Li, J. & Lou, C. Long non-coding RNA MAFG-AS1: A promising therapeutic target for human cancers. *Biomed. Pharmacother*. **163**, 114756 (2023).
33. Han, S., Chen, X. & Huang, L. The tumor therapeutic potential of long non-coding RNA delivery and targeting. *Acta Pharm. Sin B* **13** (4), 1371–1382 (2023).
34. Chao, Y. & Zhou, D. lncRNA-D16366 is a potential biomarker for diagnosis and prognosis of hepatocellular carcinoma. *Med. Sci. Monit.* **25**, 6581–6586 (2019).
35. Garcia-Padilla, C. et al. LncRNA H19 impairs chemo and radiotherapy in tumorigenesis. *Int. J. Mol. Sci.* **23** (15), 8309 (2022).
36. Wang, Y., Zhou, P., Li, P., Yang, F. & Gao, X. Q. Long non-coding RNA H19 regulates proliferation and doxorubicin resistance in MCF-7 cells by targeting PARP1. *Bioengineered* **11** (1), 536–546 (2020).
37. Akhbari, M. H., Zafari, Z. & Sheykhhasan, M. Competing endogenous RNAs (ceRNAs) in colorectal cancer: A review. *Expert Rev. Mol. Med.* **24**, e27 (2022).
38. Pan, J. et al. LncRNA JPX/miR-33a-5p/Twist1 axis regulates tumorigenesis and metastasis of lung cancer by activating Wnt/β-catenin signaling. *Mol. Cancer* **19** (1), 9 (2020).
39. Li, Q. et al. Disrupting MALAT1/miR-200c sponge decreases invasion and migration in endometrioid endometrial carcinoma. *Cancer Lett.* **383** (1), 28–40 (2016).
40. Schwarzenbach, H. & Gahan, P. B. Interplay between LncRNAs and MicroRNAs in breast cancer. *Int. J. Mol. Sci.* **24** (9), 8095 (2023).
41. Yang, Y. et al. LncRNA FTX sponges miR-215 and inhibits phosphorylation of vimentin for promoting colorectal cancer progression. *Gene Ther.* **25** (5), 321–330 (2018).
42. Ren, J. et al. Long non-coding RNA PCED1B antisense RNA 1 promotes gastric cancer progression via modulating microRNA-215-3p/C-X-C motif chemokine receptor 1 axis. *Bioengineered* **12** (1), 6083–6095 (2021).
43. Zhang, F. et al. Long non-coding RNA FTX promotes gastric cancer progression by targeting miR-215. *Eur. Rev. Med. Pharmacol. Sci.* **24** (6), 3037–3048 (2020).
44. Jiang, C. et al. lnc-REG3G-3-1/miR-215-3p promotes brain metastasis of lung adenocarcinoma by regulating leptin and SLC2A5. *Front. Oncol.* **10**, 1344 (2020).
45. Liu, C. Q. et al. MicroRNA-215-3p suppresses the growth and metastasis of cervical cancer cell via targeting SOX9. *Eur. Rev. Med. Pharmacol. Sci.* **23** (13), 5628–5639 (2019).
46. Li, X. W., Qiu, S. J. & Zhang, X. Overexpression of miR-215-3p sensitizes colorectal cancer to 5-fluorouracil induced apoptosis through regulating CXCR1. *Eur. Rev. Med. Pharmacol. Sci.* **22** (21), 7240–7250 (2018).
47. Liu, Q. P., Luo, Q., Deng, B., Ju, Y. & Song, G. B. Stiffer matrix accelerates migration of hepatocellular carcinoma cells through enhanced aerobic glycolysis via the MAPK-YAP signaling. *Cancers (Basel)* **12** (2), 490 (2020).
48. Jia, Y. et al. Phosphorylation of 14-3-3ζ links YAP transcriptional activation to hypoxic glycolysis for tumorigenesis. *Oncogenesis* **8** (5), 31 (2019).

Acknowledgements
The author thanks Scientific Research Center, The Third Affiliated Hospital of Zunyi Medical University (The First People's Hospital of Zunyi), Mrs. Xiaoqian Li, Mrs. Chengmin Deng, Mrs. Xiaoju Cheng and Dr Meng Ye for their valuable help.

Author contributions
Huang FY designed this study. Jin LY performed all the experiments. Tian YQ, Jing JM, Ya JL provided clinical tissues and prepared Figs. 1 and 2. Qing D, Jing L, Lin F and Jie W collected, analyzed, interpreted data and prepared Figs. 3 and 4. Jin LY, Jing JM and Huang FY prepared this manuscript and remain figures, including all

supply figures. All authors have read and approved the final manuscript.

Funding
The National Natural Science Foundation of China (81960506), Guizhou Provincial Basic Research Program (Natural Science) (No. Qiankehejichu-ZK[2021]488), Project for the growth of young scientific and technological talents in General Higher Education Institutions in Guizhou (No. QianjiaoheKYzi[2021]216), Science and Technology Fund project of Guizhou Provincial Health Commission(No. gzwkj2022-299), Graduate Education Innovation Program of ZMU(No. ZYK53) and Construction funding for key academic disciplines in Zunyi City and key clinical specialties in Guizhou Province.

Declarations

Competing interests
The authors declare no competing interests.

Ethics statement
Approval of the research protocol by an Institutional Reviewer Board: This study was approved by the Ethical Committee of The First People's Hospital of Zunyi (No. 2020-075).

Informed consent
Human blood samples obtained from The Third Affiliated Hospital of Zunyi medical University (The First People's Hospital of Zunyi). Written informed consent was obtained from all patients and all studies using human blood samples were approved by the The First People's Hospital of Zunyi (No. 2020-075). All animal experiments conducted was compliant with the Ethical Committee of The First Affiliated Hospital of Zunyi (No. 2021-2-28). All experiments were performed in accordance with relevant guidelines and regulations, and the study is reported in accordance with ARRIVE guidelines.

Additional information
Supplementary Information The online version contains supplementary material available at https://doi.org/10.1038/s41598-025-94638-2.

Correspondence and requests for materials should be addressed to H.-F.Y.

Reprints and permissions information is available at www.nature.com/reprints.

Publisher's note Springer Nature remains neutral with regard to jurisdictional claims in published maps and institutional affiliations.